Noise-sustained synchronization in a FitzHugh-Nagumo ring with electrical phase-repulsive coupling

Matías G. dell'Erba, Guadalupe Cascallares, Alejandro D. Sánchez and Gonzalo G. Izús

Regular Article

Noise-sustained synchronization in a FitzHugh-Nagumo ring with electrical phase-repulsive coupling

Matías G. dell'Erba[1,a], Guadalupe Cascallares[2], Alejandro D. Sánchez[1], and Gonzalo G. Izús[1]

[1] IFIMAR, Instituto de Investigaciones Físicas de Mar del Plata (CONICET–UNMDP), Facultad de Ciencias Exactas y Naturales, Universidad Nacional de Mar del Plata, Deán Funes 3350, 7600 Mar del Plata, Argentina
[2] Centro Atómico Bariloche, CONICET, San Carlos de Bariloche, R8402AGP Río Negro, Argentina

Abstract. We study the dynamical response under local noise of an excitable ring of FitzHugh-Nagumo units coupled through nearest-neighbor phase-repulsive electric synapses. The system is externally, adiabatically driven by a weak subthreshold periodic signal and independent Gaussian white noises. By varying the coupling strength and the noise intensity, two routes to noise-sustained synchronization are numerically observed and elucidated in terms of the system's non-equilibrium potential. In particular, the threshold noise intensity for synchronization is theoretically predicted and numerically confirmed.

1 Introduction

The constructive effect of noise on the dynamics of complex systems is a subject of high current interest and activity [1–3]. Examples include phenomena like coherence resonance [4], stochastic resonance (SR) [5–8] or noise-sustained synchronization in nonlinear dynamical systems [9,10]. Of particular relevance is the study of synchronization processes in populations of interacting nonlinear oscillators as a means to understand some key issues in neuroscience, where a number of modeling approaches have been based on the description of single neurons as relaxation oscillators [11].

A single neuron displays excitable behavior, in the sense that small perturbations to its quiescent state (stable stationary state of the cross-membrane potential) can lead to a large excursion of its potential before return to its rest state. This leads to unexpected nonlinear response to noise and induces in turn nontrivial behavior in the networks they may constitute. A simple example is coherence resonance, found almost two decades ago in the FitzHugh-Nagumo (FHN) model [4]. A more physiologically relevant example is the intrinsic stochastic coherence (or system size SR), first reported in reference [12], wherein the noise intensity is controlled by the system size. Important follow-up works are its application to coupled FHN-models [13] and Hodgkin-Huxley neurons [14,15]. An overview of the whole this subject can be found in reference [16].

In fact, it is well established that noise leads to various key effects in neuronal dynamics [17–19], like SR [5,12,20–22] and noise-assisted synchronization [11,23–26]. While most of the existing works have focused on the noise effects in networks connected through global or local diffusive couplings, lesser attention has been paid to phase-repulsive coupling [27–30], where the cells tend to have a phase opposite to their nearest neighbors. Antiphase coupling plays an important role in circadian oscillation in the brain [31], synthetic genetic oscillators [32], the dynamics of astrocyte cultures [33], and has been used to investigate several aspects in the dynamics of neuronal and FHN coupled models [29,30,33–35] as well as Hodgkin-Huxley neurons [36,37].

In a previous study [38] we have characterized a noise-sustained synchronization of a ring of autonomous units with excitable FHN dynamics, coupled to first neighbors in a phase-repulsive way. In particular, we have theoretically estimated the noise thresholds for activation and synchronization of an extended antiphase structure. The analysis was done in terms of the non-equilibrium potential (NEP) [39], a non equilibrium analog of a free energy which provides deep insight on the dynamical mechanisms leading to pattern formation and other phenomena where fluctuations play a constructive role [2]. More recently, a novel type of spatiotemporal SR of the antiphase state has been reported in reference [35] for a bistable FHN ring with phase-repulsive coupling, under the influence of both local and global noises. In references [35,38] 'contact'-type antiphase coupling was considered between activator components. More realistic models of synapses call to consider the (anti)diffusive 'electric' one. In this sense, it is relevant

to know to what the extent can the coupling strengths and connectivity synapses be varied so that the synchronized state remains stable. In others words, to generalize the analysis to models with more feasible couplings is a challenging problem that we try to consider here. We show that the same kind of resonance, featured with both the antiphase regular structure and the enhancement of the system's output, can be developed in a less restrictive scenario closer to the neuronal case: excitable dynamics, local noises and electrical-like synapses. In particular, we prove that the resonant dynamics can be explained in terms of noise-sustained transitions between attractors, being the adiabatic change in the attractor's relative stability – ruled by the NEP – the fundamental ingredient that drives the dynamics and determines the relevant noise scales.

The paper is organized as follows: Section 2 briefly reviews the dynamical equations of the model. Section 3 introduces the system's NEP and their limit of applicability. In Section 4 we give numerical evidence of noise-sustained synchronization and we characterize the constructive role of noise in this process. In Section 5 we elucidate the observed dynamics in terms of the corresponding NEP. The conclusions are summarized in Section 6.

2 The model

We concentrate on the physical behavior of a network of excitable elements with electrical antiphase coupling. We particularize the analysis to a FitzHugh-Nagumo (FHN) cell [4,40,41], an archetypal model of activator-inhibitor systems capable of displaying periodic oscillations, stable fixed points, and excitability [42]. This model – a two component reduction of the Hodgkin Huxley one – has been extremely useful in understanding the dynamics of some neural [43] and cardiac tissues [44], to cite a few examples of biomedical relevance. We consider a ring of N identical excitable FHN cells with electrical phase-repulsive nearest-neighbor coupling, and submitted to a common subthreshold signal and independent additive Gaussian white noises. The equations for the model are:

$$
\begin{aligned}
\dot{u}_i = {} & b\, u_i \left(1 - u_i^2\right) - v_i + S(t) - E\left[(u_{i+1} - u_i)\right.\\
& \left. + (u_{i-1} - u_i)\right] + r_1\, \xi_i^{(u)}(t) + r_2\, \xi_i^{(v)}(t) \\
\dot{v}_i = {} & \epsilon\left(\beta\, u_i - v_i + C\right) + r_3\, \xi_i^{(u)}(t) + r_4\, \xi_i^{(v)}(t), \quad (1)
\end{aligned}
$$

where the activator u_i is the fast variable which mimics the action potential off cell i and the inhibitor v_i is the slow – or recovery – variable which is related to the time dependent conductance of the potassium channels in the membrane [45]. Here $i = 1, \ldots, N$; $u_{N+1} \equiv u_1$, $u_0 \equiv u_N$, $S = A_0 \sin \Omega t$ is the external signal, ϵ is the activator-inhibitor time scales ratio, while $E > 0$ is the coupling strength. Throughout the work the following values have been adopted: $N = 256$, $\epsilon = \beta = 0.01$, $b = 0.035$, $C = 0.02$, $A_0 = 0.011$, $\Omega = 0.002$, $\epsilon\, r_1 = r_3 = \cos 0.05$ and $\epsilon\, r_2 = r_4 = \sin 0.05$. The values of the parameters are not totally arbitrary: Ω is such that the period

$T = 2\pi/\Omega$ remains larger than the typical deterministic time (i.e. the turnaround time of a single spike), so that the signal can be regarded as an adiabatic perturbation. Similarly, some parameters were selected in such a way that they satisfy an integrability condition required by the theoretical characterization of the dynamics (see next section). Finally, for the statistical properties of the Gaussian noises $\xi_i^{(u,v)}$ we assume $\langle \xi_i^{(p)}(t)\rangle = 0$ and $\langle \xi_i^{(p)}(t)\, \xi_j^{(q)}(t')\rangle = \eta\, \delta_{i,j}\, \delta_{p,q}\, \delta(t - t')$, where η is the common noise intensity and $p, q \in \{u, v\}$.

Equations (1) include a direct electrical connection between cells (gap junction). Note that the coupling term is inhibitory-like: when neuron i fires, neuron $i \pm 1$ are less likely to fire. Inhibitory coupling is a basic ingredient in the dynamics of neocortical pyramidal neurons [46], cortical networks [47] and play a major role in the dynamics of synchronous neural firing [48].

3 The non-equilibrium potential

The NEP Φ can be considered as the nonequilibrium analog of a free energy. It is an appropriate Lyapunov functional of the deterministic dynamics that provides information on the local and global properties of attractors. It characterizes their (linear and nonlinear) stability and also determines the height of the barriers separating attraction basins, which in turn define the transition rates among the different attractors. For Langevin-type dynamics, Graham [39] has defined Φ through the zero-noise limit of the logarithm of the stationary probability density function

$$
\lim_{\eta \to 0} P^{\text{stat}}\left(\mathbf{W}, \eta\right) = Z\left(\mathbf{W}\right) \exp\left[-\frac{\Phi(\mathbf{W})}{\eta} + \mathcal{O}(\eta)\right], \quad (2)
$$

where $\mathbf{W}$ are the variables of the problem. From a technical point of view, this definition presents an advantage over the purely deterministic Lyapunov function: since noise is present from the outset, the extra freedom in the choice of the transport matrix can render in some cases the problem integrable [49]. That is precisely the case for some versions of the FHN model in the bistable and excitable regimes [50,51]. For adiabatic external signal and linear coupling in the activator variables, we have shown that the NEP is the sum of two terms: the first one is determined by the potential of the isolated nodes – a local component that includes the driving – while the second one (nonlocal) is determined by the topology of the network and results to be a quadratic form in the network's activator variables, with the adjacency matrix as kernel [52]. Integrability conditions – arising from the NEP's derivation – restrict the range of validity of the NEP's expression. In particular, the linear coupling is restricted to be symmetric. Nevertheless, we remark that bistable and excitable dynamics can be reached within the aforementioned restriction. For electrical antiphase coupling the NEP takes
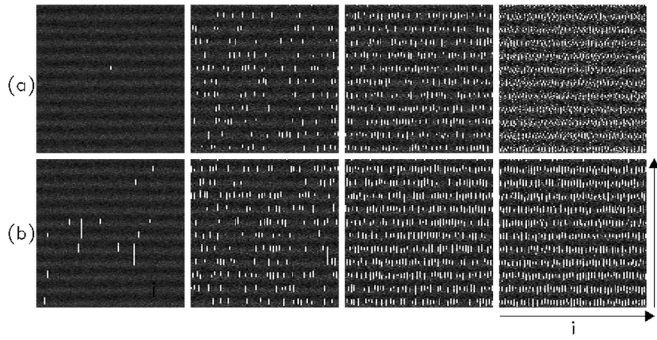
Fig. 1. Time-evolution of the u-component for a subset of 100 cells, for different noise intensities η and phase repulsive coupling E. Time runs on the vertical direction, for approximately 11 signal periods. White represents activated neurons, and black inhibited ones. (a) $E = 0.006$ and $\eta = 2 \times 10^{-7}$, $4 \times 10^{-7}, 6 \times 10^{-7}, 1.2 \times 10^{-6}$ (from left to right); (b) $E = 0.007$ and $\eta = 2 \times 10^{-7}, 4 \times 10^{-7}, 6 \times 10^{-7}, 8 \times 10^{-7}$ (from left to right).

the form:

$$\Phi(\mathbf{u}, \mathbf{v}) = \sum_{i=1}^{N} \left[\Phi_s\left(u_i, v_i\right) + \frac{2E}{\lambda_1}\left(u_i u_{i+1} - u_i^2\right) \right], \quad (3)$$

$$Z(\mathbf{u}, \mathbf{v}) = \text{const.}, \quad (4)$$

with Φ_s the NEP for a single cell [50] given by:

$$\Phi_s(u_i, v_i) = \frac{\epsilon}{\lambda_2}\left(v_i^2 - 2\beta\, u_i v_i - 2C v_i\right) + \frac{2\lambda\epsilon}{\lambda_1\lambda_2}(\beta\, u_i^2 + 2C u_i)$$
$$- \frac{2}{\lambda_1}\left[\frac{b}{2}u_i^2 - \frac{b}{4}u_i^4 + S(t)\, u_i\right], \quad (5)$$

where $\lambda_1 = r_1^2 + r_2^2$, $\lambda_2 = r_3^2 + r_4^2$ and $\lambda = r_1 r_3 + r_2 r_4$. Integrability conditions also constrain the parameters to obey

$$\beta\lambda_1 + \lambda_2/\epsilon = 2\lambda, \quad (6)$$

a condition satisfied only below the Hopf bifurcation. Notice the parametric dependence of Φ on t, caught up by each u_i variable through its coupling to the adiabatic external signal.

4 Noise-sustained synchronization

We numerically observe the synchronization of the network with the external signal for appropriate values of noise and coupling strengths. To have an overview of the dynamics, in Figure 1 we present the activity record of $\{u_i\}$ for a subset of neurons for some values of E and η. For vanishingly small noise intensities, only small-amplitude homogeneous subthreshold oscillations around the rest state can be appreciated. This coherent behavior is induced by the adiabatic signal and represents the rest state, for which $u_i(t) \approx u_j(t)$. As the noise intensity increases, so does the number of cells that become noise-activated
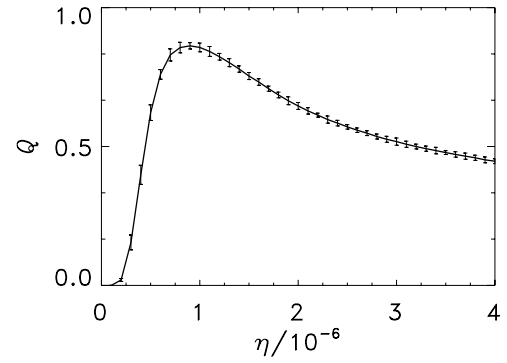

Fig. 2. Q-factor vs. noise intensity (averaged over 20 realizations on a network of 256 cells) for phase repulsive coupling $E = 0.007$ and $nT = 131\,989$. Error bars are magnified by a factor of 4 to render an appreciable picture.

during roughly half a cycle of the external signal and the system starts to synchronize (we call *active* those cells for which $u_i(t)$ exceeds some threshold value u_{th}).

As expected, we verify that as one neuron activates, in general it inhibits its nearest neighbors. The outcome of this phenomenon is the antiphase state (APS) that partially appears along the ring during the stage of noise-activation. For higher levels of noise, the cells' activity becomes highly synchronized with the external signal. In this scenario noise plays a constructive role and the synchronization becomes eventually degraded for larger values of noise intensities. To illustrate and quantify this point we introduce the Q-factor

$$Q = \sqrt{Q_{\sin}^2 + Q_{\cos}^2}, \quad (7)$$

with

$$Q_{\sin} = \frac{1}{nT}\int_0^{nT} 2Ac(t)\sin(\omega t)dt$$

$$Q_{\cos} = \frac{1}{nT}\int_0^{nT} 2Ac(t)\cos(\omega t)dt.$$

Here n is the number of periods T covered by the integration time and we have introduced the normalized global activation

$$Ac(t) = \frac{1}{N}\sum_{i=1}^{N} \theta[u_i(t) - u_{\text{th}}], \quad (8)$$

where θ is the Heaviside step function. As expected, $Ac(t)$ is not sensitive to u_{th} for reasonable values of threshold, so hereafter we fix $u_{th} = 0.39$. By normalization, $Ac = 1/2$ corresponds to a state where half of the neurons remain activated. However, in an APS the Ac does not reach the value $1/2$ because alternance fails due to the local noise, a necessary ingredient for activation. The failure takes the form of defects where pairs of neighbor neurons remain inhibited or excited.

In Figure 2 we show Q as a function of η for $E = 0.007$. A maximum of Q at $\eta \sim 10^{-6}$ can be appreciated. This curve indicates that there is an optimal noise level at an

Fig. 3. Time-evolution of the u-component for a subset of 50 cells, for different noise intensities η and coupling E. The parameters are: $E = 0.0095$ and $\eta = 1.6 \times 10^{-7}$ (a), 2.8×10^{-7} (b), 6×10^{-7} (c), 10^{-6} (d).
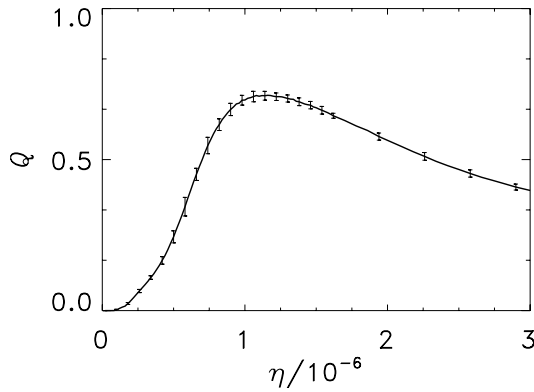
Fig. 4. The same as Figure 2 for coupling $E = 0.0095$.

Fig. 5. NEP landscape in the (u_1, u_2) plane for the reduced two-neuron system (in units of 10^{-6}), for signal $S = 0$, phase repulsive coupling $E = 0.007$ and along the $v_i = \beta u_i + C$ lines. The associated nullclines are shown in dotted and dashed lines. The level-line ticks indicate the Φ-gradient direction. The lines correspond to the levels: -17.5, -16.4, -14.806502 (saddle), $-12, -6$ and 0. Some of them are labeled in the figure.

intermediate noise strength for neuronal coherence and signal enhancement. At that noise intensity, the system reaches the best synchronization.

A different synchronization scheme is numerically observed for larger values of E, as we show in Figure 3 for $E = 0.0095$. In this case, for appropriate values of noise, a stationary APS is developed where the activated state is macroscopically occupied and almost half of the neurons remain excited. Since activation is noise-mediated, this kind of pattern (induced in principle by the spatial coupling) has defects that break the alternance. Both structure and defects are persistent in time as can be observed in Figure 3b: the resulting structure is shown as a stripe pattern for the activity record. Finally, in Figure 3d we show the evolution for the synchronized state for $\eta = 10^{-6}$. The activity's synchronization with the signal is clear. Note that this case has two characteristical levels of noise, one for activation and the other one for synchronization.

In Figure 4 we show for $E = 0.0095$ the Q-factor as a function of the noise intensity. The curve aspect is similar to the one in Figure 2, but in this case the best performance is observed at $\eta \sim 1.2 \times 10^{-6}$.

5 Theoretical description of the dynamics

As in reference [38], a theoretical study of the dynamics can be done by exploiting the properties of the NEP during the time-evolution. We consider a reduced two-neuron
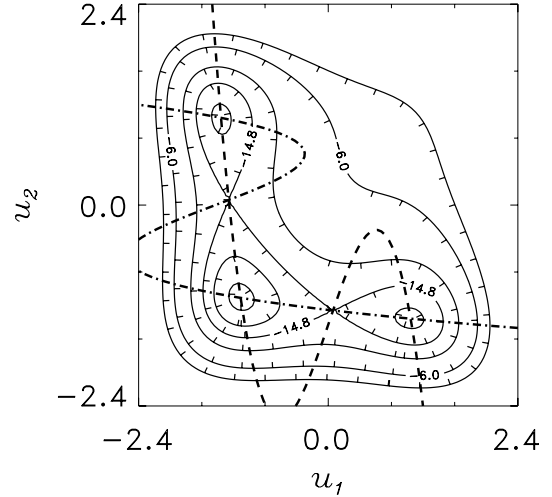
system of variables (u_1, u_2, v_1, v_2), which is a minimal description of an idealized case where all the even nodes on one hand, and all the odd nodes on the other, have the same stochastic phase-space trajectory. For this effective model, the NEP in equation (3) take the simple form:

$$\Phi(\mathbf{u}, \mathbf{v}) = \Phi_s(u_1, v_1) + \Phi_s(u_2, v_2) \\ + 2E(2u_1 u_2 - u_1^2 - u_2^2)/\lambda_1. \quad (9)$$

We first analyze the case of small coupling: Figure 5 displays the Φ-level curves in the (u_1, u_2) plane, in the absence of signal for $E = 0.007$. Here, the $\{v_i\}$ have been adjusted to the slow manifolds $v_i = \beta u_i + C$ to include all the fixed points in the same two-dimensional scheme. Both the attractors and the saddles can be obtained, either from the intersection of the nullclines or by minimizing $\Phi(u_1, u_2, v_1, v_2)$. Besides the uniform rest state (which lies along the line $u_1 = u_2$), two (excited) attractors and two saddle points can be appreciated. Note that the NEP and their fixed points distribution are symmetric with respect to the $u_1 = u_2$ line, reflecting the u_1–u_2 permutation invariance of the dynamical equations. The complete equivalence between symmetric points in the reduced model originates a degeneration in the antiphase state (u_1 activated, u_2 inhibited or u_2 activated, u_1 inhibited).

The global stability is given by the depth of each attractor's well respect of the saddle level, and this difference depends on $S(t)$. To illustrate this point, in Figure 6 we show Φ as a function of S for the uniform state (labeled by u), for the saddle (indicated by s), and for the activated state (indicted by a). Here $|S| \leq A_0$ and for each value of S, the global stable state corresponds to the attractor(s) with the lowest value of Φ, while the other ones are either metastable or unstable states.
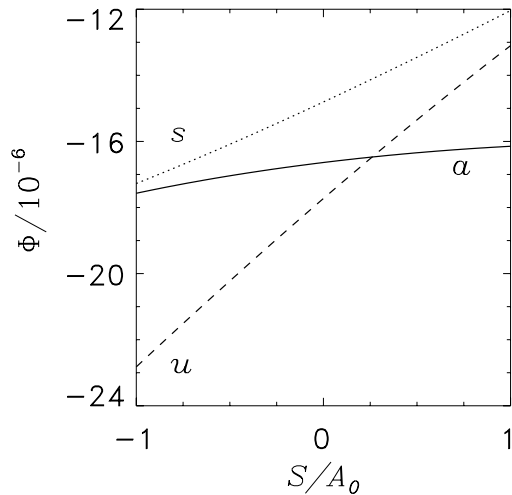
Fig. 6. Dependence of the NEP value on the scaled signal at the saddle s, activated a and uniform u states, for a two-neuron system with coupling $E = 0.007$. Note that both saddle points share the same value of Φ (the same stands for the activated states).
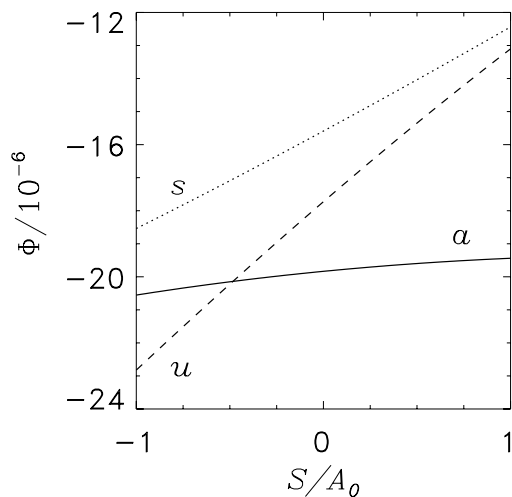

Fig. 7. The same barrier scheme of Figure 6 for coupling $E = 0.0095$.

For $S = A_0$ the difference in Φ between s and u is $\Delta\Phi_s = 1.06 \times 10^{-6}$. For a noise level of this order, the two-cell system would climb that potential barrier and transit to the excited state, that has a lower Φ value. For this noise level the APS can return to the u-state because the barrier at $S = -A_0$ is significantly smaller than the first one. In fact, $\eta \sim \Delta\Phi_s$ is the expected order of magnitude of noise for full synchronization, in good agreement with the numerical results of Figure 2.

The alternative route to synchronization observed for larger values of coupling can also be elucidated in terms of the NEP. While the NEP's landscape has the same qualitative structure than in Figure 5, the dependence of the potential barriers with the external signal changes: Figure 7 shows Φ as a function of S for the uniform u, saddle s and the activated state a for $E = 0.0095$. In this

case, the difference in Φ between s and u for $S = A_0$ is $\Delta\Phi_a = 6.6 \times 10^{-7}$. For a noise level of this order, the two-cell system would climb the potential barrier and transit to the activated state, that has a lower Φ value. In this excited states, the NEP's barrier between s and a goes from $\Delta\Phi = 7 \times 10^{-6}$ at $S = A_0$ to $\Delta\Phi = \Delta\Phi_s = 2.01 \times 10^{-6}$ at $S = -A_0$. Hence, as S varies the system remains confined in a, which explains the observed robustness of the excited state (see Figs. 3b and 3c). The noise level must increase one order of magnitude to transit again to u. In fact, $\eta \sim \Delta\Phi_s$ estimates the optimal level of noise to return to the uniform state, so completing the cycle. This noise-sustained decay is also associated with a decrease in Φ. For $\eta \sim \Delta\Phi_s$, the barrier $\Delta\Phi_a$ is not significant and the system easily reaches an excited state during each oscillation of the external signal, namely, it synchronizes (see Fig. 3d).

The two-cell approximation does not take into account the eventual formation of defects, which break the background activation's alternance of extended APS, as can be observed in Figures 3b and 3c. Being these theoretical results approximate, we remark that they elucidate the route to synchronization and also allow to estimate the order of magnitude for the relevant scales of noise.

6 Conclusion

We have investigated the stochastic dynamics of a ring of electrical phase-repulsive-coupled FitzHugh-Nagumo cells, externally forced by a common subthreshold harmonic signal, and submitted to additive and independent Gaussian white noises of the same intensity η.

We numerically observe that local additive noise is able to sustain an extended antiphase structure (APS) where the cells change alternately their state of activation. This APS can be also synchronized with an external subthreshold adiabatic signal for appropriate parameter values.

The observed resonance, featured with both the antiphase regular structure and the enhancement of the system's output was recently reported in reference [35] for bistable FHN rings with antiphase coupling and local and global noise. We have proved here that the same kind of structure can be developed in a less restrictive scenario closer to the neuronal case: excitable dynamics, local noises and electrical-like synapses.

We remarks that the constructive role of noise as an essential input to the stochastic synchronization process is encoded with the measure of the coherence Q-factor, i.e. equation (7), which exhibits a maximum as a function of the noise intensity η. The role of the noise is thus twofold: it induces the phenomenon but also enforces it. This fact reminds one the phenomenon of double SR [53].

To elucidate the numerical results we have considered the system's non-equilibrium potential (NEP). In particular, we have studied a reduced model with two coupled cells, whose NEP allows for a theoretical characterization of the dynamics. The reduced system has five fixed points, which are NEP's critical points. The minima of the NEP (i.e., the attractors) are a uniform (rest) state, and two

activated states where one neuron remains excited and the other one inhibited. The system has moreover two unstable points (NEP's saddle points) which separate the uniform state from the excited ones. By analyzing the potential barriers and their dependence with the external signal amplitude, we have shown that the dynamics can be explained in terms of noise-sustained transitions between these attractors. In particular, two potential barriers organize the dynamics: the first one corresponds to macroscopic activation (i.e, transition from the uniform state to the antiphase one) while the second barrier corresponds to the decayment from the activated state to the uniform one. The noise scale for full synchronization is estimated with the largest barrier. We remark that all the decays are noise-induced and correspond to global decrease of the NEP, being the role of the signal to change adiabatically the relative stability between the wells, so providing the route to synchronization. This is the fundamental ingredient that drives the dynamics and determines the noise level for synchronization.

The integrability condition arising from the NEP's derivation restricts the range of validity of its expression. Although bistable and excitable dynamics can be reached within the aforementioned constraint, self-sustained oscillatory dynamics remain outside the range of parameters. Nevertheless, within the range, the NEP appears as a powerful theoretical tool to analyze stochastic dynamics. Our results are expected to depend on both temporal and/or spatial noise correlations, as occurs (for example, in coupled FHN systems) for related phenomena like coherence resonance [9]. The NEP approach could be useful even in those cases since dynamics driven by space correlated and colored (Ornstein-Uhlenbeck) noises can be described –in principle– in terms of their corresponding NEP [54]. The explicit dependence of the NEP on the adjacency matrix also suggests that the same approach would be useful for analyzing other kinds of synchronization (or self-organization phenomena) in complex networks and continuous systems. In this sense, we hope that the NEP approach can be used to understand phenomena and properties of the system which are not obvious outside of this framework.

References

1. J. García-Ojalvo, J.M. Sancho, *Noise in Spatially Extended Systems* (Springer-Verlag, New York, 1999)
2. F. Sagués, J.M. Sancho, J. García-Ojalvo, Rev. Mod. Phys. **79**, 829 (2007)
3. R. Toral, C.J. Tessone, J. Viana Lopez, Eur. Phys. J. Special Topics **143**, 59 (2007)
4. A.S. Pikovsky, J. Kurths, Phys. Rev. Lett. **78**, 775 (1997)
5. L. Gammaitoni, P. Hänggi, P. Jung, F. Marchesoni, Rev. Mod. Phys. **70**, 223 (1998)
6. K. Wiesenfeld, F.J. Jaramillo, Chaos **8**, 539 (1998)
7. T. Wellens, V. Shatokhin, A. Buchleitner, Rep. Prog. Phys. **67**, 45 (2004)
8. H.S. Wio, Phys. Rev. E **54**, R3075 (1996)
9. C. Zhou, J. Kurths, Phys. Rev. Lett. **78**, 775 (1997)
10. C.J. Tessone, A. Scirè, R. Toral, P. Colet, Phys. Rev. E **75**, 016203 (2007)
11. A. Pikovsky, M. Rosenblum, J. Kurths, *Synchronization: a Universal Concept in Nonlinear Sciences* (Cambridge University Press, 2003)
12. G. Schmid, I. Goychuk, P. Hänggi, Europhys. Lett. **56**, 22 (2001)
13. R. Toral, C.R. Mirasso, J.D. Gunton, Europhys. Lett. **61**, 162 (2003)
14. G. Schmid, P. Hänggi, Physica A **325**, 165 (2003)
15. M. Wang, Z. Hou, H. Xin, Phys. Lett. A **334**, 93 (2005)
16. G. Schmid, P. Hänggi, Math. Biosci. **207**, 235 (2007)
17. B. Lindner, J. García-Ojalvo, A. Neiman, L. Schimansky-Geier, Phys. Rep. **392**, 321 (2004)
18. D.T. Kaplan, J.R. Clay, T. Manning, L. Glass, M.R. Guevara, A. Shrier, Phys. Rev. Lett **76**, 4074 (1996)
19. J.R. Clay, J. Comput. Neurosci. **15**, 43 (2003)
20. B. Lindner, J. García-Ojalvo, A. Neimann, L. Schimansky-Geier, Phys. Rep. **392**, 321 (2004)
21. P. Hänggi, ChemPhysChem **3**, 285 (2002)
22. P. Jung, J.W. Shuai, Europhys. Lett. **56**, 29 (2001)
23. T. Yanagita, T. Ichinomiya, Y. Oyama, Phys. Rev. E **72**, 056218 (2005)
24. A.M. Lacasta, F. Sagués, J.M. Sancho, Phys. Rev. E **66**, R045105 (2002)
25. L. Callenbach, P. Hänggi, S.J. Linz, J.A. Freund, L. Schimansky-Geier, Phys. Rev. E **65**, 051110 (2002)
26. J.A. Freund, L. Schimansky-Geier, P. Hänggi, Chaos **13**, 225 (2003)
27. S.K. Han, C. Kurrer, Y. Kuramoto, Phys. Rev. Lett. **75**, 3190 (1995)
28. D. Postnov, S.K. Han, H. Kook, Phys. Rev. E **60**, 2799 (1999)
29. E.I. Volkov, E. Ullner, J. Kurths, Chaos **15**, 023105 (2005)
30. C.J. Tessone, E. Ullner, A.A. Zaikin, J. Kurths, R. Toral, Phys. Rev. E **74**, 046220 (2006)
31. L. Yan, N.C. Foley, J.M. Bobula, L.J. Kriegsfeld, R. Silver, J. Neurosci. **25**, 9017 (2005)
32. E. Ullner, A. Zaikin, E.I. Volkov, J. García-Ojalvo, Phys. Rev. Lett. **99**, 148103 (2007)
33. G. Balázsy, A. Cornell-Bell, A.B. Neimal, F. Moss, Phys. Rev. E **64**, 041912 (2001)
34. A. Sherman, J. Rinzel, Proc. Natl. Acad. Sci. USA **89**, 2471 (1992)
35. Q. Zhao, C.G. Yao, M. Yi, Eur. Phys. J. B **84**, 299 (2011)
36. Y. Li, G. Schmid, P. Hänggi, L. Schimansky-Geier, Phys. Rev. E **82**, 061907 (2010)
37. X. Ao, G. Schmid, P. Hänggi, Math. Biosci. **245**, 49 (2013)
38. G. Izús, A. Sánchez, R. Deza, Physica A **388**, 967 (2009)
39. R. Graham, in *Instabilities and Nonequilibrium Structures*, edited by E. Tirapegui, D. Villarroel (D. Reidel, Dordrecht, 1987), pp. 271–290
40. R. FitzHugh, Biophys. J. **1**, 445 (1961)
41. J.S. Nagumo, S. Arimoto, S. Yoshizawa, Proc. IRE **50**, 2061 (1962)

42. J.A. Acebrón, A.R. Bulsara, W.-J. Rappel, Phys. Rev. E **69**, 026202 (2004)
43. C. Koch, *Biophysics of Computation: Information Processing in Single Neurons* (UP, New York, 1999)
44. *Theory of Heart*, edited by L. Glass, P. Hunter, A. McCulloch, (Springer-Verlag, Berlin, 1991)
45. N.B. Janson, A.G. Galanov, E. Schöll, Phys. Rev. Lett. **93**, 010601 (2004)
46. A. Destexhe, M. Rudolph, J.-M. Fellous, T.J. Sejnowski, Neuroscience **107**, 13 (2001)
47. N. Brunel, X.J. Wang, J. Comput. Neurosci. **11**, 63 (2003)
48. C. van Vreeswijk, L.F. Abbott, G.B. Ermentrout, J. Comput. Neurosci. **1**, 313 (1994)
49. H.S. Wio, R.R. Deza, Eur. Phys. J. Special Topics **146**, 111 (2007)
50. G. Izús, R.R. Deza, H.S. Wio, Phys. Rev. E **58**, 93 (1998)
51. S. Bouzat, H.S. Wio, Phys. Lett. A **247**, 297 (1998)
52. A. Sánchez, G. Izús, Physica A **389**, 1931 (2010)
53. A. Zaikin, J. García-Ojalvo, R. Báscones, E. Ullner, J. Kurths, Phys. Rev. Lett. **90**, 030601 (2003)
54. A. Schenzle, T. Tél, Phys. Rev. A **32**, 596 (1985)